Spatio-temporal control over destabilization of Pickering emulsions stabilized by light-sensitive dextran-based nanoparticles

Valentin Maingret, Véronique Schmitt, Valérie Héroguez

Spatio-temporal control over destabilization of Pickering emulsions stabilized by light-sensitive dextran-based nanoparticles

Valentin Maingret [a,b], Véronique Schmitt [a,]*, Valérie Héroguez [b,]*

[a] Centre de Recherche Paul Pascal, UMR 5031, Univ. Bordeaux, CNRS, 115 avenue du Dr Albert Schweitzer, 33600 Pessac, France.

[b] Laboratoire de Chimie des Polymères Organiques, Univ. Bordeaux, CNRS, Bordeaux INP, UMR 5629, Bordeaux, 16 Avenue Pey-Berland, F-33607 Pessac, France.

*corresponding authors
veronique.schmitt@crrp.cnrs.fr
heroguez@enscbp.fr

Abstract

The implementation of light-sensitive Pickering emulsions with spatio-temporal responsiveness in advanced applications like drug-delivery, colloidal or reaction engineering would open new avenues. However, curiously, light-sensitive Pickering emulsions are barely studied in the literature and their biocompatibility and/or degradability scarcely addressed. Thus, their development remains a major challenge. As an original strategy, we synthesized light-sensitive nanoparticles based on biocompatible Poly(NitroBenzylAcrylate) grafted dextran (Dex-g-PNBA) to stabilize O/W Pickering emulsions. The produced emulsions were stable in time and could undergo time and space-controlled destabilization under light stimulus. Irradiation time and alkaline pH-control of the aqueous phase were proved to be the actual key drivers of destabilization. As the nanoparticles themselves were photolyzed under light stimulus, possible harmful effects linked to accumulation of nanomaterials should be avoided. In addition to UV light (365 nm), visible light (405 nm) was successfully used for the spatio-temporal destabilization of the emulsions, offering perspectives for life science applications.

Keywords: Stimuli-responsive Pickering emulsions, light-responsive particles, natural polysaccharide, on-demand release, photolysis, photo-induced coalescence

1. Introduction

Stimuli-responsive Pickering emulsions are of high interest for the design of smart systems (Dupont et al., 2021; Maingret et al., 2020; Tang et al., 2015). In this respect, light-sensitive trigger remains one of the most convenient switches because it is non-invasive and easy to set up. It is also the most challenging system to obtain. One reason may lie in the fact that many energy dissipative phenomena can happen in an enlightened emulsion: multi scattering and refraction for instance. That is why the response of the Pickering emulsion stabilizers must be as fast and efficient as possible, to lower the required light intensity and irradiation time. Overcoming such challenges is worth investigation as these systems have enormous potential as tools for controlled-delivery, colloidal engineering or reaction catalysis (Chen et al., 2014; Xie et al., 2017). While offering great stability in time, they can be destabilized on-demand like other stimuli-responsive systems. In addition, light can be switched on/off as an external stimulus and be precisely focused in space. Thus, light stimulus enables a spatio-temporal control over the response of the system. Very few examples of such systems can be found in the literature and most of them imply the use of non-degradable inorganic stabilizers (Bai et al., 2016; Jiang et al., 2016), which may hinder the future development of such systems in fields where bio-compatibility or (bio)degradation are required (Ren et al., 2019). Physical or chemical modification of bio-based materials is needed to provide photo-responsiveness, compared to some naturally light-sensitive inorganic materials like TiO_2. In this respect, many photo-sensitive groups with reversible or irreversible response can be found in the literature and thus could be used as Pickering emulsion stabilizer modifiers like nitrobenzyl derivatives, which are well known as cleavable units under UV light (365 nm) (H. Zhao et al., 2012). Specifically, Soliman et al. grafted a polyNitroBenzylAcrylate (PNBA), a photo-sensitive and

hydrophobic polymer, onto dextran, a biocompatible and biodegradable hydrophilic natural polysaccharide (Soliman et al., 2016). They were then able to elaborate nanoparticles *via* nanoprecipitation. They observed that the photo-cleavage of PNBA to produce Poly(Acrylic Acid) (PAA) led, at a higher scale, to the photolysis of the PNBA grafted dextran (Dex-g-PNBA) nanoparticles (El Founi et al., 2018; Soliman, 2018; Soliman et al., 2019). As another example, the use of PNBA as surface modifier of stabilizing cellulose nanocrystals has been recently presented in the work of Tajmoradi et al. (Tajmoradi et al., 2021). However, light stimulus was used prior to emulsification and did not induce the destabilization of the emulsion. Zhao et al. and Zeng et al. employed alginate and cyclodextrin for the design of light-sensitive Pickering emulsion stabilizers and are thus part of the only examples which promote the use of bio-friendly brick materials. They both used photoisomerization of azobenzene derivatives to induce the disassembly of their particles based on host-guest interactions with cyclodextrin (Zeng et al., 2019; X. Zhao et al., 2021). In this work, we present an original strategy to formulate for the first time Pickering emulsions stabilized by light-sensitive particles based on PNBA-grafted dextran. The purpose was to prove that such nanoparticles could stabilize Pickering emulsions, but also that their photolysis under UV light (365 nm) could lead to the coalescence of the droplets and the destabilization of the Pickering emulsion. As a result, Pickering emulsions were successfully obtained with an average drop size governed by the nanoparticle concentration (as a result of the limited coalescence phenomenon). Then, irradiation time and alkaline pH of the continuous phase were proved to be the key elements for the destabilization of these Pickering emulsions. To widen the scope of applications, visible light (405 nm) was also used to induce the space-controlled destabilization of the Pickering emulsions in an alkaline medium. In this case, destabilization took more time to occur than with UV irradiation but remained fast (< 2h), mainly because of the lower energy of the visible irradiation compared to UV light. This

strategy, combining both temporal and spatial control over the coalescence process opens interesting perspectives: Pickering emulsion droplet reactors, on-demand release, colloidal and reaction engineering.

2. Experimental section

2.1. Materials

Dextran (M_w = 34,000 g/mol, M_n = 24,000 g/mol, Đ = 1.4 as measured by the authors using size-exclusion chromatography (SEC)) and dodecane (99%) were purchased from ABCR. All used solvents were of analytical grade.

2.2. Synthesis of Dex-g-PNBA

Dex-g-PNBA was synthesized following previous works from Soliman et al. (Soliman, 2018; Soliman et al., 2014). Briefly, dextran was modified with alkyne moieties to operate a click-chemistry reaction with azide end-chain modified Poly(NitrobenzylAcrylate) (PNBA) (**Figure S1**). On one side, NBA monomer was synthesized from o-nitrobenzyl alcohol and acryloyl chloride (Eq.I, FigureS1) then polymerized through Single Electron Transfer- Living Radical Polymerization (SET-LRP) using ethyl 2-bromoisobutyrate as initiator (Eq.II, Figure S1). Finally, bromide end-chain was modified thanks to sodium azide (Eq.III, Figure S1). On the other side, modification of dextran (Eq. V, Figure S1) was performed through esterification of the hydroxyl moieties with activated 5-hexynoic acid. Full details on the synthesis products and their characterization by ^{1}H NMR (400 MHz NMR instrument Bruker 400 UltraShield), FTIR, and SEC can be found in the supporting information section (**Figure S1-S10**). Final grafting of PNBA to modify dextran was checked and quantified thanks to SEC measurements.

2.3. Dex-g-PNBA nanoparticles obtained by nanoprecipitation

Dex-g-PNBA nanoparticles (NPs) were obtained through nanoprecipitation using a syringe pump (CHEM- YX Fusion 101 Syringe Pump). Specifically, Dex-g-PNBA chains were dissolved in a 20 mL mix of THF/H_2O (90/10 v/v) (3 g/L) and injected in a 40 mL water bath (non-solvent) at 0.4 mL/min. At the end of this process, further 40 mL of water were added to the dispersion. THF was then removed with rotary evaporator (30°C bath). The resulting aqueous dispersion was poured in a cellulose dialysis bag with 100 kDa pore size. 5 liters of water were used as counter-dialysis solution and were changed after 6, 12 and 24 hours. Finally, the recovered dispersion was concentrated using a rotary evaporator (40 °C bath) to eliminate water. The mass concentration of nanoparticles into dispersions was determined using the residual dry weight technique. The dispersions can be stored for several months without stability issues. HITACHI H-600 Transmission Electron Microscopy (TEM) instrument (HV=75 kV) was used for the shape characterization of the nanoparticles. The volume-averaged diameter D[4,3] of nanoparticles was calculated from TEM pictures using ImageJ software as follows (eq.1):

$$D[4,3]=\frac{\sum_{i}^{n} d_i^4}{\sum_{i}^{n} d_i^3} \quad (1)$$

where d_i is the diameter of a nanoparticle from an n-nanoparticles population ($n \geq 200$). NanoZS90 Dynamic light scattering (DLS) instrument (Malvern Instrument Ltd, UK) was used at a scattering angle of 90° to characterize the size distribution of the nanoparticles after dilution in water and their average diameter (z in nm). Three measurements of 10 runs (30 s each) at 25°C were carried out unless otherwise noticed. The concentration of the sample was set low enough to avoid multiple scattering and is given when necessary. Polydispersity index (PDI) was computed by the instrument and is expressed as follows (eq.2):

$$PDI=\left(\frac{\sigma}{z}\right)^2 \quad (2)$$

Where z is the average diameter (nm) and σ the typical standard deviation (nm) of the sample. DLS allows a reliable statistically significant measure of the nanoparticle size in the suspension.

2.4. Formulation of O/W Pickering emulsions

Emulsions volume was set to 4 mL using water phase/oil phase (dodecane) ratio of 50/50 to initially assess the type of emulsion. This 50/50 volume ratio was chosen to determine the preferred emulsion type (O/W or W/O) dictated by the particles without interaction from the composition. For all other experiments the water/oil ratio was fixed to 80/20 v/v. Thanks to dry weight technique results, a precise amount of nanoparticles could be introduced in the water phase. This quantity was computed as a concentration relative to the volume of the oil dispersed phase. Nanoparticles were not dispersible in the oil phase, but since the total interfacial area, S, to be stabilized by the nanoparticles is directly linked to the dispersed oil volume, $V_{d,}$ and to the drop size, D[3,2] through $S=6V_d/D[3,2]$, it is more logical to compare the amount of particles to the one of oil. Dispersion of oil into the aqueous suspension was operated thanks to an Ultra Turrax (IKA T25) with a shaft (S25N 10G) at 20 000 rpm for 2 minutes. First, formulation of Pickering emulsion was done at a water phase/oil phase ratio of 50/50 v/v to assess the kind of emulsion stabilized by the nanoparticles (O/W or W/O). For that, after emulsification, droplets from the emulsion were put in two different vials containing either water or oil. The aliquots diluted easily into water, not in oil, proving that in all cases direct oil-in-water (O/W) Pickering emulsions were obtained. In all this work, only O/W Pickering emulsions were obtained, and the water phase/oil phase ratio used in the following was always set to 80/20 v/v. An optical microscope (Zeiss Axioskop 40) in bright field using x5 and x10 objectives was employed to observe the emulsions and pictures were taken using a digital camera device linked to the microscope. Size measurements of at least

two hundred drops when possible were obtained by analysing the pictures using the ImageJ software. Such a high amount of drops allows to get a statistical significance. The mean drop size of the emulsions was computed according to the Sauter diameter (eq.3):

$$D[3,2]=\frac{\sum_{i}^{n} d_i^3}{\sum_{i}^{n} d_i^2} \quad (3)$$

where d_i is the diameter of a drop from a n-drops population. The Sauter diameter is defined as the surface-average diameter of the drops. Finally, to describe the drop size distribution width of the emulsions, a typical standard deviation σ_d was calculated.

2.5. Light-induced destabilisation of O/W Pickering emulsions

2.5.1 Nanoparticles photolysis

Nanoparticle dispersions were loaded in a DLS cuvette and diluted to reach 0.2 mg/mL. A tiny stirring bar was added to ensure homogenization during the irradiation process. UV irradiation was performed with a LIGHTNINGCURE® series apparatus from HAMAMATSU equipped with a light guide and a 365 nm wavelength filter. The DLS cuvette was placed at a 3 cm distance (center-to-center) of the light guide. Irradiance, determined using a Power Puck II radiometer from EIT® was usually equal to approximately 140 mW/cm^2 unless otherwise noticed. Regular DLS acquisitions were performed to measure the size distribution of the nanoparticles. Three measurements of 6 runs (10 s each) were taken to ensure data reliability. Derived Count Rate (DCR) signal was also acquired and used for analysis. DCR depends both on the radius of the nanoparticles (r) and their concentration (c_p) (Eq.4):

$$DCR \propto c_p * r^6 \quad (4)$$

If the size distribution remains unchanged, the DCR is directly proportional to the concentration (calibration curve can be found in the supporting information section (**Figure S11)**). In the photodegradation experiments, it was then possible to quantify the relative decrease of the nanoparticle amount when their size did not change with time by normalizing all DCR values by the one obtained at t_0. However, it happened that the average size of nanoparticles increased in time, meaning that the DCR value measured may be higher than expected. In these cases, as the DCR always still decreased with irradiation time, the normalization allowed to major the relative population of nanoparticles meaning that the amount of remaining particle is then overestimated. Degradation of the nanoparticles was considered as complete when the relative amount of nanoparticles was equal or lower than 10%. From that point, no additional measurement nor irradiation step was done. Absorption scans in UV-visible light of irradiated samples were carried out using a Cary 100 UV-visible Spectrophotometer from Agilent Technologies. The samples were diluted by a factor three with pure water before analysis. Absorbance at 265 nm (indicating presence of nitrobenzyl acrylate moieties) and at 325 nm (indicating presence of nitrosobenzaldehyde moieties) were extracted from the scans.

2.5.2 Time and space O/W Pickering emulsion destabilization

In order to observe the destabilization under optical microscopy, a tiny part of a Pickering emulsion cream was deposited into a quartz slide (4.5 cm per 1.2 cm) with a small cuvette (3.8 cm per 0.8 cm, 0.1 cm deep) that was then filled with various aqueous phases. The hollow quartz slide was then recovered with a flat quartz lamella of the same size. Capillary forces made the slide and the lamella sticking together and ensured sample preservation with time. Then, the same conditions as for the nanoparticle photolysis were applied, that is 3 cm (center-to-center) between the light guide and the sample and an irradiance of about 140 mW/ cm^2. The impact of the continuous phase pH was studied by using various aqueous phases in

the quartz cuvette. Coalescence of the emulsion droplets was observed thanks to an optical microscope in bright field using a x5 objective. To irradiate the sample with visible light, a fluorescence microscope with an integrated 50 mW blue laser (405 nm) at 70% of its power intensity was used. The irradiation was focused on a precise area of the sample and regular pictures were taken. To assess the presence of nanoparticles at the interfaces, cryo-SEM was performed on emulsion droplets without irradiation and after a long irradiation time. Dodecane-in-water emulsion were formulated with a nanoparticles suspension where the amount of particles was set to 3 mg/mL of oil without control over the pH of the continuous phase. Cryo-SEM allowed direct observation of the samples without the use of a replica.

3. Results and discussion

3.1. Dex-g-PNBA synthesis

Dextran was modified with alkyne moieties and grafted with PNBA-N_3 chains thanks to a click-chemistry reaction (**Figure 1**). According to SEC and ^{1}H NMR measurements, PNBA block length was about 7000 g/mol (DP = 33) and 12 grafts over 100 glucosidic units of a dextran chain could be found in average (**Figure S10**). As a result, Dex-g-PNBA chains were composed of 83%wt of PNBA in average. Complete characterizations of the different products obtained through the different synthesis steps can be found in the supporting information section (**Figure S1-S10**).

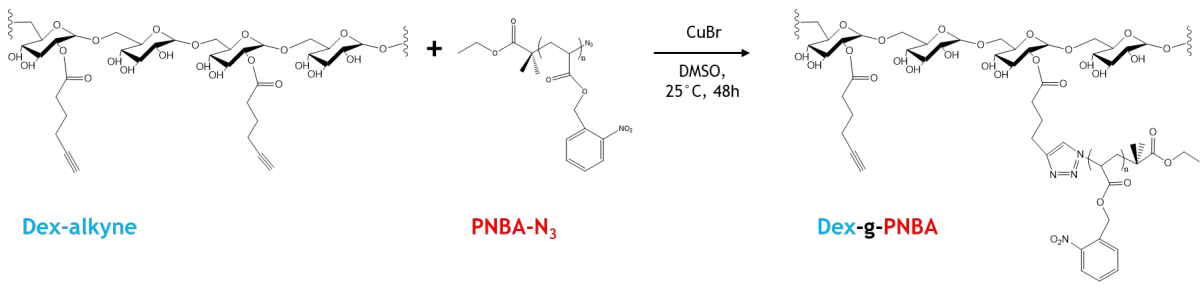

Figure 1. Scheme representing the grafting of PNBA photo-sensitive polymer onto modified dextran thanks to a copper catalyzed click-chemistry reaction.

3.2. Dex-g-PNBA nanoparticles

Nanoparticles obtained *via* nanoprecipitation were characterized thanks to TEM observations, assessing their spherical shape (Figure 2). Size distribution of the Dex-g-PNBA nanoparticles from DLS and from TEM pictures analysis were determined in addition to their zeta potential without and in presence of salt (Table 1). As a result, nanoparticles exhibit spherical shape and possess a narrow monomodal size distribution (PDI < 0.2). In absence of salt, they are negatively charged (ζ < -20 mV), however these charges can be easily screeened by slightly increasing the ionic strength of the medium (10 mM NaCl). It can be seen that this increased ionic strength made the nanoparticles size distribution a little bit broader and centered on bigger size which may be the result of partial swelling or slight aggregation. The effects of the ionic strength and so of the zeta potential of the nanoparticles on the stabilization of Pickering emulsions are discussed in the next section.

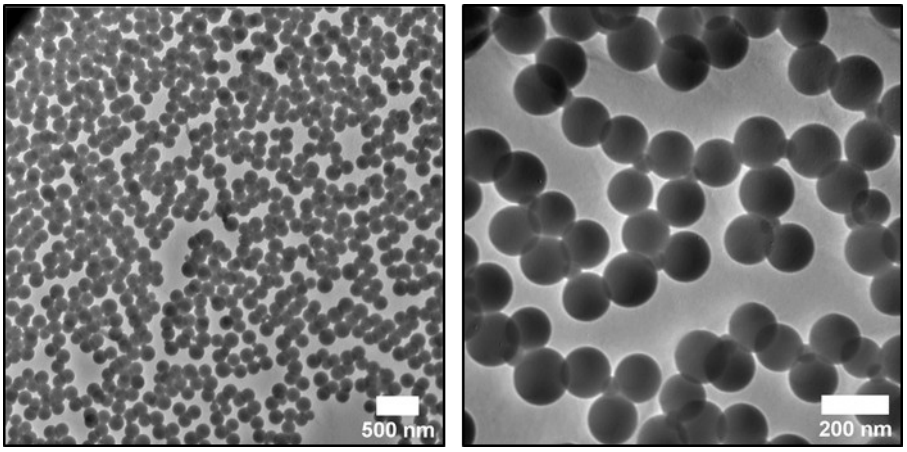

Figure 2. TEM images of Dex-g-PNBA nanoparticles.

Table 1. Size distributions and Zeta potential of the Dex-g-PNBA nanoparticles.

	Diameter (TEM)	Diameter (DLS 90°)	Zeta Potential and Electrophoretic mobility
NPs without salt	156 ± 17 nm PDI = 0.01	122 ± 33 nm PDI = 0.07	ζ = -28 mV μ_p = - 2.2 µmcm.V^{-1}s^{-1}
NPs with 10 mM salt	-	174 ± 74 nm PDI = 0.18	ζ = -6 mV μ_p = - 0.5 µmcm.V^{-1}s^{-1}

NPs with 30 mM salt	-	320 ± 183 nm PDI = 0.33	ζ ~ 0 mV

After full characterization, nanoparticle dispersions were stored hidden from the light in a cupboard. They could be stored for more than 3 months without any stability issue (**Figure S12**).

3.3. Formulation of O/W Pickering emulsions

3.3.1. Determination of emulsion type

Water phase/oil phase ratio 50/50 v/v Pickering emulsions were first formulated to assess the type of obtained emulsion: O/W emulsions were always formed. Because of the large diameter of the droplets and the low density of dodecane (0.75 $g.cm^{-3}$) compared to water, all emulsions creamed quickly. In the following water phase/oil phase ratio used was always 80/20 v/v.

3.3.2. Influence of ionic strength in the formulation step

As seen before, ionic strength influences the zeta potential of the particles. To evaluate the impact of the latter on Pickering emulsion characteristics, Pickering emulsions at a nanoparticle concentration of 0.8 mg/mL were formulated without and with 10 mM carbonate buffer (pH 10). As a result, the emulsion droplets stabilized without the presence of salt were much bigger (around 650 μm) than the one from the emulsion with 10 mM of salt (436 μm) (Figure 3). Moreover, it was observed that the subnatant of the first emulsion (without salt) was far more bluish than the second one (which was rather clear). Thus, it indicated that not all the nanoparticles took part in the stabilization process, probably owing to the charges they bear which made them too hydrophilic so that a part of the nanoparticles remained in the aqueous continuous phase. More salt (30 mM) led to a slight further decrease of the droplet size (383 μm) but it induces rapid aggregation because of the very low zeta potential of the

nanoparticles (~ 0mV). In the following, 10 mM of carbonate buffer (pH 10) were systematically introduced for the formulation step to increase the amount of nanoparticles involved in the stabilization of interfaces. It can be noticed that the emulsified creamed volume represents 33% of the total sample volume (see figure S14) showing that the drops are randomly close packed in the cream (between 64 and 65 %v/v). This is in complete agreement with the optical microscopy picture (Figure 3) showing noninteractive drops.

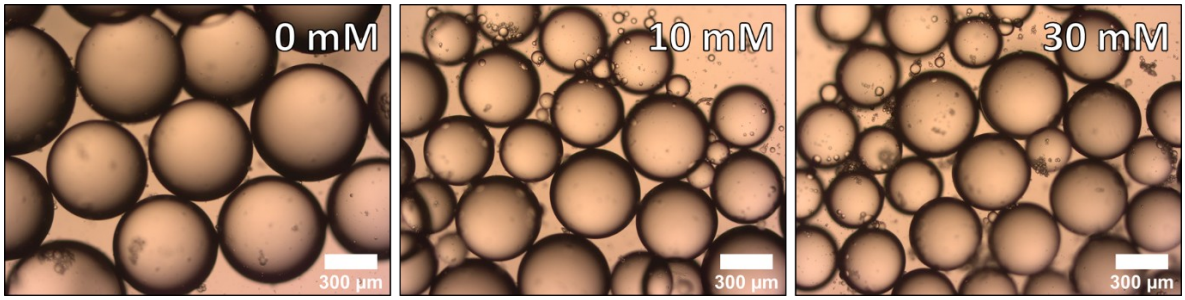

Figure 3. Droplets of emulsion obtained at 0.8 mg/mL of nanoparticles at different ionic strength values (0, 10 and 30 mM of pH 10 buffer).

3.3.3. Influence of nanoparticle concentration – limited coalescence phenomenon

Coalescence is usually an unwanted deleterious phenomenon leading to the emulsion destabilization. However, in Pickering emulsions, a so-called limited coalescence phenomenon happens right after the homogenization step and is, on the contrary, beneficial. Indeed, the emulsification step produces a large excess of interfacial area compared to the area that can be covered by the stabilizing nanoparticles. Consequently, drops, which are not enough covered, coalesce to decrease the interfacial area. This coalescence phenomenon stops when the drops are sufficiently covered (stabilizing particles are irreversibly anchored at the interface). Thus, one can take benefit from this phenomenon to produce a narrow monomodal size distribution of droplets with great reproducibility despite the turbulent flow that has been used for emulsification. Limited coalescence generally happens in the low-particle concentration range and in this case, for geometrical reasons, the inverted Sauter diameter of

the emulsion droplets is linearly related to the amount of nanoparticles used to stabilize them, as described in eq. 5 (Schmitt et al., 2014):

$$\frac{1}{D[3,2]} = \frac{c_p}{4 C \rho_p d_p} \quad (5)$$

where c_p is the concentration of particles relative to the volume of the dispersed phase, C is the surface coverage, that is, the fraction of the droplet interfacial area covered by the particles, ρ_p is the particle density and d_p is the stabilizing particle diameter. Various O/W Pickering emulsions were formulated by varying the concentration of nanoparticles relative to the volume of the oil phase. In our case, optical microscopy observations confirmed that the average diameter of the droplets linearly decreased when increasing the amount of particle up to a concentration of 7 mg/mL showing that limited coalescence phenomenon is operative in these Pickering emulsions **(Figure 4)**. Detailed measured sizes of Pickering emulsions are given in the Supporting Information section (**Figure S13**). This allowed varying the drop size from 55 to 623 µm (more than a decade) keeping a narrow drop size distribution. For the following induced destabilization experiments we chose to set the nanoparticles concentration equal to 2.4 mg/mL of oil.

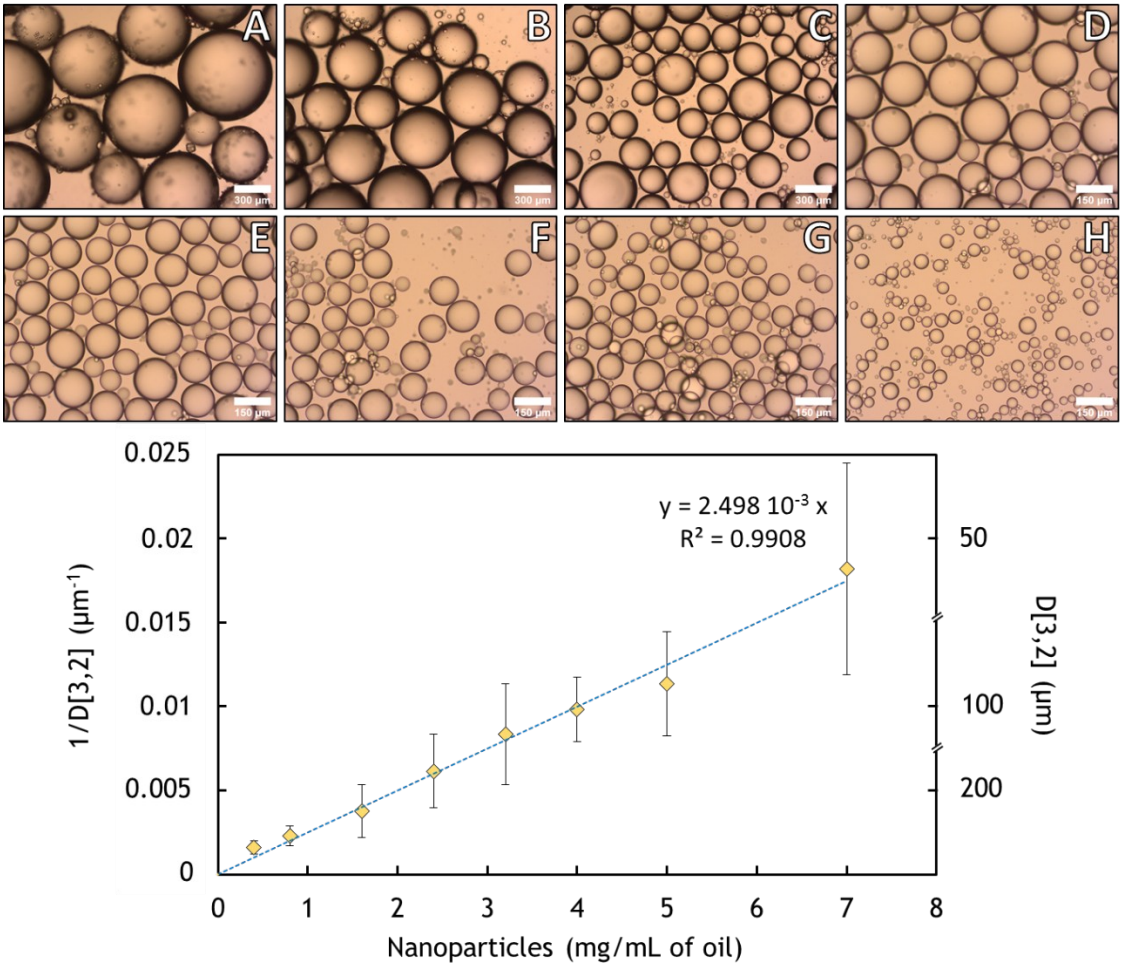

Figure 4. Optical microscopy pictures of emulsions with various nanoparticle concentrations with respect to oil from 0.4 (A) to 7 mg/mL (H), scale bar is equal to 300 μm for samples from A to C and to 150 μm for samples from D to H (top). Evolution of 1/D[3,2] as a function of the nanoparticle concentration with a linear fit (bottom).

Pickering emulsions were stored in the same conditions as the stabilizing nanoparticles (protected from light). Various emulsions formulated at different nanoparticle concentrations showed good stability at room temperature for more than 5 months (**Figure S14**).

3.4. Light-induced destabilization of O/W Pickering emulsions

NBA moieties of Dex-g-PNBA chains are sensitive to UV light (λ =365 nm) as described in the literature (Soliman et al., 2016). Thus, under irradiation, NBA units are photo-cleaved to release nitrosobenzaldehyde (NSBZ) and to generate acrylic acid units (AA) on the grafts

(**Figure S15**). Soliman et al. showed that these AA units could be deprotonated in presence of phosphate buffer saline (PBS) (Soliman et al., 2019). This dramatically increased their solubility in water so that irradiated Dex-g-(NBA-co-AA) chains became also much more soluble, leading to the destabilization of the nanoparticles. Our goal was then to design such nanoparticles able to both stabilize and destabilize O/W Pickering emulsion by exposure of the emulsion to a light stimulus providing photolysis of nanoparticles. In a process of understanding the multi-scale phenomena that happen, we first investigated the degradation of the nanoparticles in aqueous dispersions. Influence of irradiation time and alkaline pH on the kinetics of degradation were studied. Then, light controlled destabilization of Pickering emulsions was studied. The question was to determine whether or not controlled coalescence of the Pickering emulsions could be achieved in alkaline media despite the various dissipation phenomena that can lead to a loss of light intensity.

3.4.1. Photolysis of Dex-g-PNBA nanoparticles

UV irradiation (at 365 nm) was used to degrade the nanoparticles in aqueous dispersions. Nanoparticle aqueous dispersions of initially 0.2 g/L were prepared in a DLS cuvette with a little stirrer. Various aqueous conditions were tested: pure water, 10 mM NaCl, 10 mM buffered solution at pH 9 and 10, and 10 mM NaOH. The samples were placed at 3 cm (center-to-center) from the UV source and stirred to homogenize the dispersion (UV spot was placed at mid-height). Then, at regular irradiation times, size distributions and DCR values were obtained from DLS to quantify the relative amount of nanoparticles remaining as a function of irradiation time (Figure 5**A**). No control over the pH of the dispersion (pure water, 10mM NaCl) resulted in an incomplete degradation (~80%) of the nanoparticles after 20 minutes (1200 s) of irradiation. Longer irradiation time would maybe not be enough to fully degrade the nanoparticles as the results showed a plateau-like tendency. On the other side, in

alkaline conditions, complete degradation (> 90%) was achieved after only 5 minutes of irradiation. Detailed final values of degradation can be found in the supporting information section (**Figure S16**).

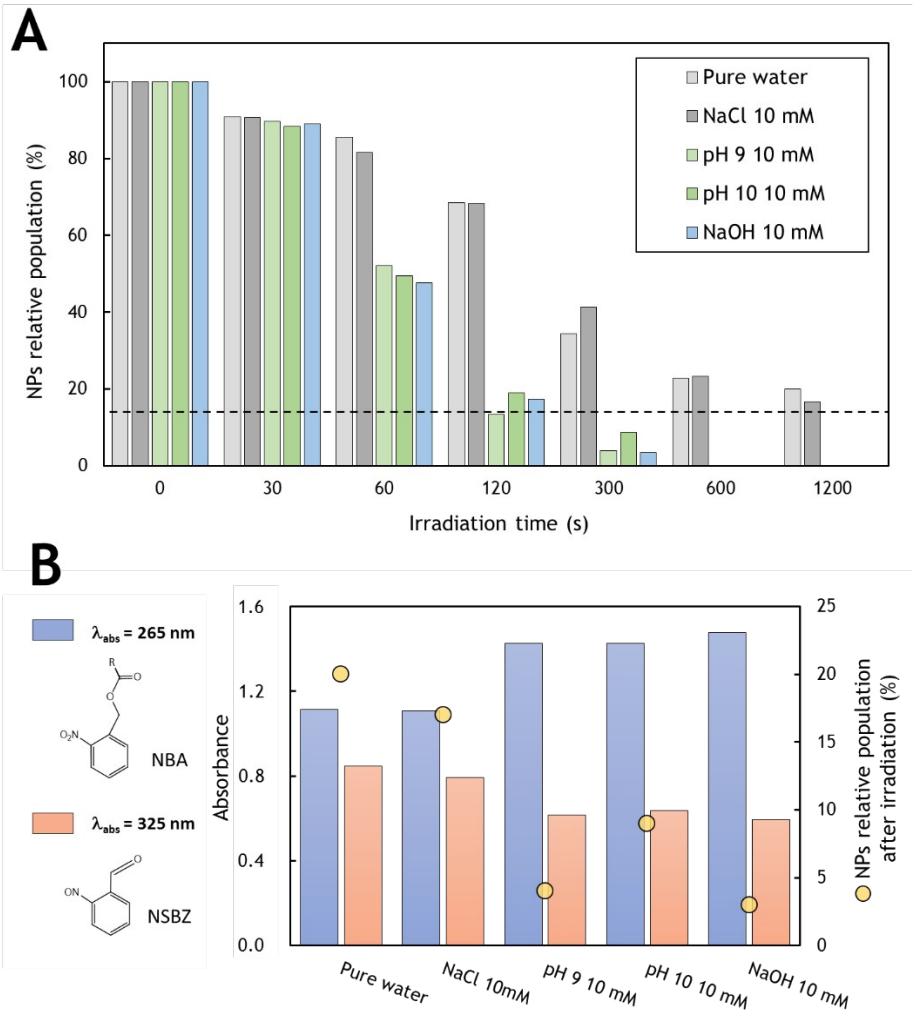

Figure 5. Degradation of nanoparticles as a function of irradiation time with an initial concentration of 0.2 g/L in different aqueous media. Dotted line represents the 10% threshold below which the degradation was considered as complete (detection threshold) (A). Absorbance of the irradiated samples at 325 nm (related to the presence of NSBZ) and at 265 nm (related to the presence of NBA). Irradiation time was set to 20 min for the first two samples and to 5 min for the three others (B).

To investigate this different behavior depending on the aqueous conditions, absorptions of NBA units and NSBZ units (at 265 nm and 325 nm respectively) were determined (Figure 5**B**) thanks to UV-vis spectroscopy measurements on diluted irradiated samples in their final state. These two absorption peaks are closely related, as the photo-cleavage of one NBA unit

produces one unit of NSBZ. For pure water and NaCl 10 mM, where the irradiation time was the longer (20 min vs 5 min for the others), the absorption of NBA and NSBZ were lower and higher respectively than those from other experimental conditions, which was expected. However, although the photo-cleavage was more advanced in these two cases, the photolysis of the nanoparticles was lower (Figure 5**A**). In the other samples where the pH conditions were alkaline, faster and complete photolysis (>90%) were obtained (5 min). In addition, the UV-vis results showed that the obtained absorbance of NSBZ units in such samples (directly related to the photo-cleavage advancement) were lower compared non-alkaline conditions. This is consistent with the lower irradiation time, but it also means that the photo-cleavage of NBA moieties is not the kinetically determinant step as nanoparticles could be better photolyzed at lower photo-cleavage rates. The pH of the medium, as well as the irradiation time are then synergic key parameters as they settle the maximum nanoparticle achievable photolysis efficiency. Finally, another sample with a 10 mM buffer at pH 9 was irradiated at half the used irradiance (70 mW/cm^2) (**Figure S16-S17**). Results showed that the degradation was initially slower but still exceeded 90% after 5 minutes meaning that irradiance may be lowered without a high loss of performances. However, to balance the possible light dissipative phenomena in emulsions, we chose to keep the irradiance at 140 mW/cm^2 for the following section.

3.4.2. Light-induced Pickering emulsion destabilization

3.4.2.1. Under UV-light (λ = 365 nm)

From the previous part, it has been shown that nanoparticle degradation can be performed up to 80% after 20 minutes of irradiation in a non-controlled pH medium. Transposed into a Pickering emulsion system, a degradation of 80% of the stabilizing nanoparticles should reasonably lead to coalescence events and likely to the full destabilization of the emulsion.

Two different experiments were carried out to verify this hypothesis. First, a freshly made Pickering emulsion without controlled pH was subjected to UV irradiation for 2 hours. Release of NSBZ was assessed but no destabilization could be observed after more than a week. It then proved that the destabilization could not be easily achieved without control over the pH of the emulsion. This sample and a control emulsion (not irradiated) were both observed by Cryo-SEM. Nanoparticles anchored at the interface of droplets could be seen in the control sample (**Figure S18**) whereas surprisingly no one could be observed at the surface of the irradiated droplets (**Figure S19**). Thus, it meant that irradiated emulsions could remain stable even without particles stabilizers (it should be noticed that an initial emulsion prepared without nanoparticles was not stable). This behavior suggests that a secondary stabilization, post-irradiation occurred and hindered the coalescence. Another Pickering emulsion without controlled pH was subjected to UV irradiation for 2 hours under high stirring (which did not affect the emulsion stability) so that the subnatant became orange (evidencing the presence of NSBZ). After one night, the emulsion remained still stable as in the first experiment. Part of the subnatant (whose pH was equal to 4.7) was discarded and replaced with NaOH to adjust the pH to 12. In less than 5 minutes coarse coalescence happened under no further agitation than a slight homogenization. Finally, after 30 minutes, a full demixion of the two phases was observed (**Figure S20**). Again, this behavior could be explained by a secondary stabilization mechanism, post-irradiation, coming from protonated AA units produced during the irradiation step. Indeed, in addition to incomplete degradation of nanoparticles (as found out in the previous part), poorly soluble protonated PAA grafts may adsorb on the oil droplets and provide steric stabilization of these (Figure 6). When the pH is adjusted to higher values, the PAA chains became deprotonated and much more soluble into water, leading to their desorption and to bare droplets that coalesced. The coalescence can be then induced by the

light if the pH of the emulsion is initially alkaline enough. Reciprocally, an emulsion whose pH is not controlled can become pH-sensitive after irradiation.

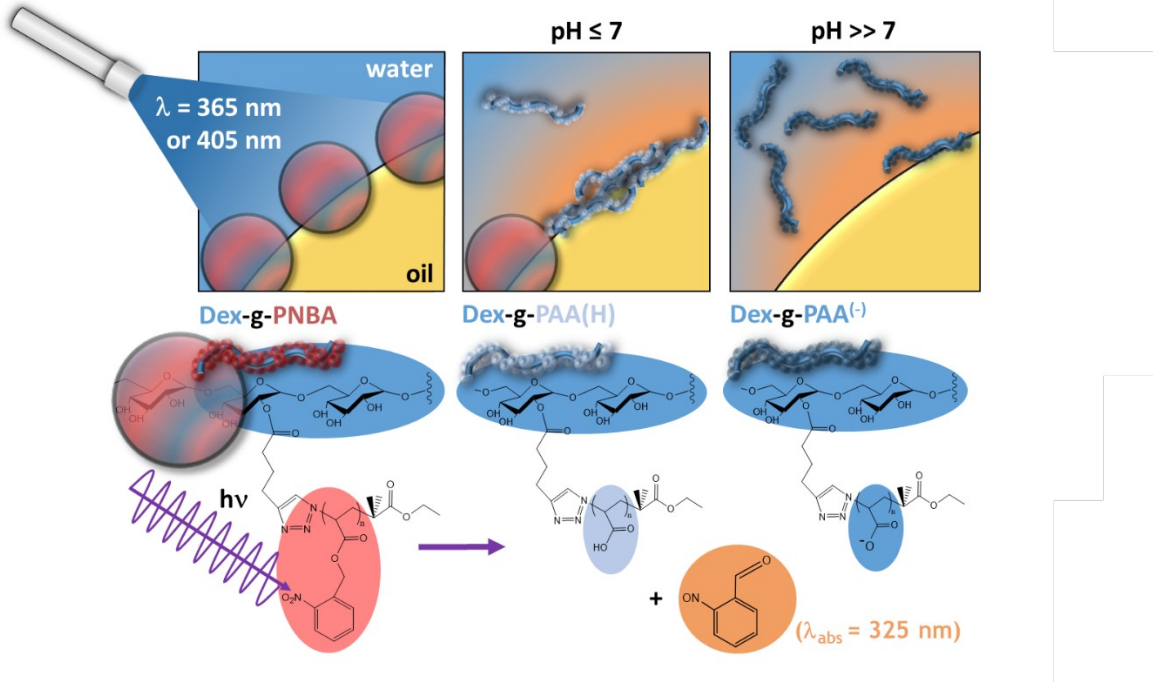

Figure 6. Destabilization of an O/W Pickering emulsion under irradiation depending on the pH conditions.

In addition to irradiation time and intensity, pH could be wisely used to control the destabilization of the formulated Pickering emulsions: from partial to complete coalescence of the droplets.

In another set of irradiation experiments, emulsion cream was poured into a quartz cuvette lamella and water phase was added to fill it. In a first approach, NaOH 1M was taken as continuous phase to ensure quick solubilization of the PAA grafts produced during irradiation. Despite the high molarity and pH of the environment, the droplets of emulsion remained stable. Direct observation, under optical microscope, of the coalescence events of the droplets under irradiation was made (Figure 7). Time-lapse of this destabilization experiment can be found in the supporting files (**Video S1**).

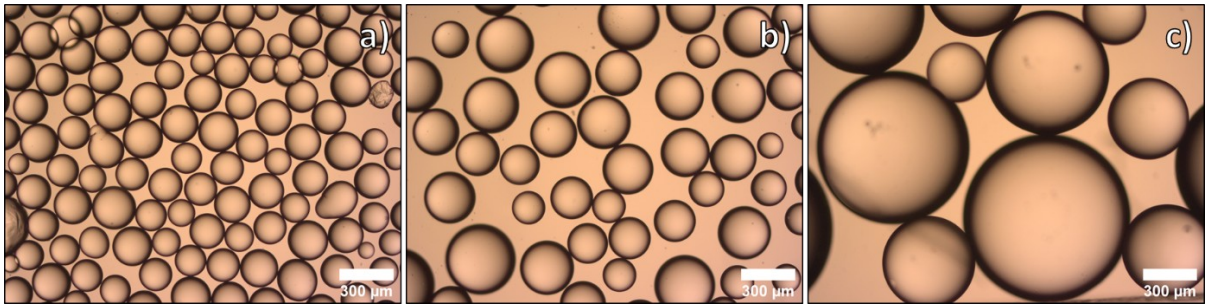

Figure 7. Optical microscopy pictures of the droplets in 1M NaOH before irradiation (nanoparticle concentration was 2.4 mg/mL of oil) a), after 5 min of irradiation at 140 mW/cm^2 b) and after very gentle agitation of the irradiated sample c).

The coalescence events started quite quickly (90 secs) and ended after 5 minutes of irradiation likely because after some coalescence events, drops are no more at contact as required for coalescence to happen. To substitute motion that was absent due to the drops large size and confinement, the sealed cell was slightly stirred (low upside downs of the sealed quart lamellae). Then droplets easily coalesced into much bigger ones. Finally, instead of NaOH at 1M, an aqueous pH 10 buffer at 100 mM was used and also led to coalescence (data not shown). To better evidence the space control coalescence that could be achieved, the quartz lamellae system containing an emulsion was partially covered with an aluminum sheet and then irradiated. After 30 minutes, a clear difference could be observed between the covered and uncovered area (Figure 8). In addition, the transition area which delimits the two parts showed that a great spatial resolution was achieved.

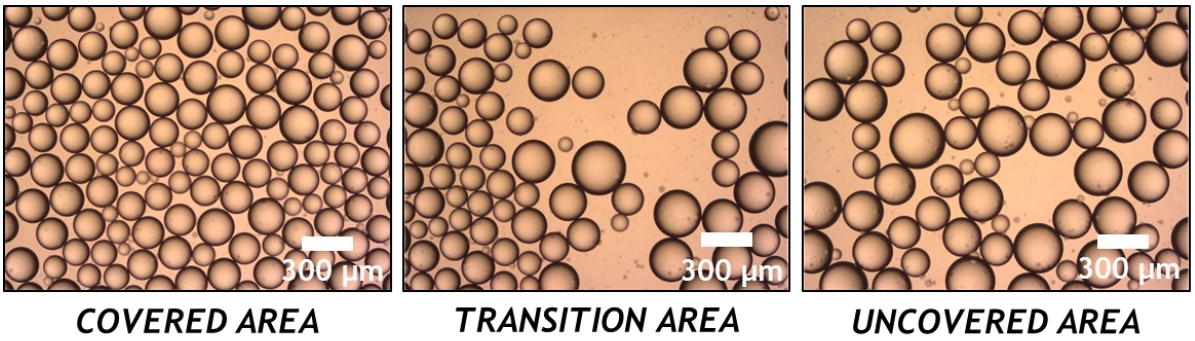

Figure 8. Optical microscopy pictures of a Pickering emulsion subjected to a space-controlled irradiation. Pictures from the covered to the uncovered areas from left to right were taken after 30 minutes of irradiation. Emulsion was formulated at 2.4 mg/mL of nanoparticles and the continuous phase was composed of 100 mM pH 10 buffer. Left part of the sample was kept protected from UV

light (left picture), right part was exposed (right picture). The picture in the middle focuses on the limit between covered (left part of the picture) and uncovered (right part of the picture). Left part of these pictures is unaffected while the right part shows a loss of droplets and an increase of the drop size.

D[3,2] of the droplets in the covered and the uncovered area of the sample were computed from 200 droplets. Without irradiation, the size distribution of the droplets did not change at all from 169 ± 37 μm. On the irradiated side, clear destabilization of the droplets can be observed. Mean size increased and size distribution broadened to reach 227 ± 67 μm. Oil volume conservation during the process implies that in average almost 3 droplets of 169 μm coalesced together to produce one droplet of 227 μm. However, some of them did not coalesce at all, mainly due to the absence of homogenization which may be necessary to make droplets coalesced together as seen before (**Figure 7**).

3.4.2.2. Under visible light (λ = 405 nm)

Light responsiveness of nitrobenzyl derivatives is induced around 365 nm. This wavelength may be slightly shifted depending on the added modifying groups (H. Zhao et al., 2012). In the work of Del Campo et al. visible light (λ = 411 nm) was successfully used to induce the light response of nitrobenzyl derivatives (Del Campo et al., 2005). However, no other example on the use of visible light could be found in the literature. In order to widen the range of applications of our system, we tried to use visible blue light (405 nm) to photo-cleave, for the first time, NBA moieties and thus induce the destabilization of the Pickering emulsions. As before, 1M NaOH was used to dilute the emulsion cream into the quartz cuvette lamella. The laser beam was focused on a specific area of the sample (dot square on **Figure 9**) for 100 minutes and regular pictures of this irradiated area were taken. No destabilization due to the highly alkaline outer phase (which was not irradiated) was evidenced even after 100 minutes of observation (**Figure 9**). As a result, only the area which was subjected to the irradiation showed signs of destabilization (coalescence). Because of the coalescence events, some

droplets moved so that they also took part later in the local coalescence phenomenon, although they were not initially in the region of interest. Destabilization took nearly 30 more minutes to occur than when with the UV source, this may be due to the lower energy of the photons (at 405 nm vs at 365 nm) but also from the intrinsic lower power of the laser from the fluorescence microscope (50 mW, 70% intensity).

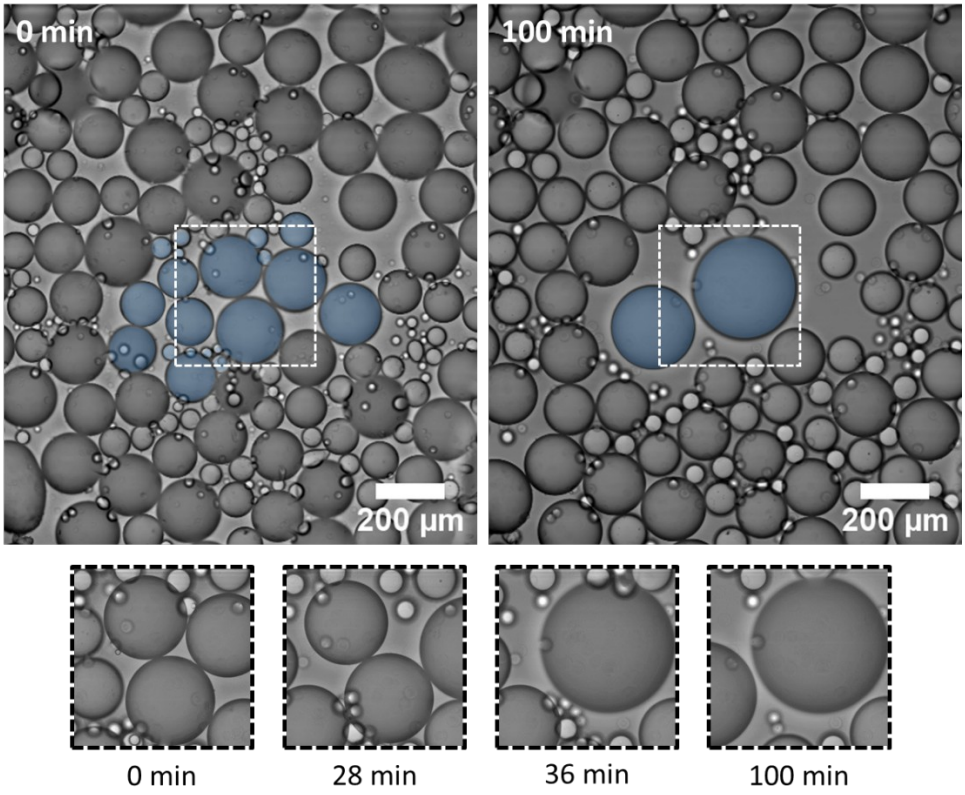

Figure 9. Optical microscopy pictures of the sample at different times of irradiation with a 405 nm source from a fluorescence microscope. The irradiation was focused in the white dot square and the droplets which coalesced are coloured in blue. Main coalescence events and times are shown in the little inserts. Pickering emulsion was formulated at a nanoparticle concentration of 2.4 mg/mL of oil.

Oil volume conservation during the process was assessed by computing the total volume of the 21 blue droplets at t_0 and of the 2 blue droplets at t_{100min}. After comparing the values, an error of less than 3% was found, evidencing the conservation of the oil volume during the process and that all the droplets which coalesced were well identified (**Figure S21**). This interesting result gives a proof of concept for the use of this system as micro-droplet reactors which can be merged on demand and with a high spatial precision using visible light.

4. Conclusion

This work offers a proof of concept of the use of Dex-g-PNBA as a brick material for the design of Pickering emulsion stabilizers. Stable O/W Pickering emulsions with droplets of tunable and narrow size distribution could be obtained. Photo-responsiveness of the polymer, at larger scale of the nanoparticles and at an even larger scale of stabilized Pickering emulsion were assessed and studied. As a result, additionally to irradiation, control over the pH of the continuous phase allows enhancing the light-response of the nanoparticle dispersion and of the Pickering emulsions. Finally, precise time and space control over coalescence of the Pickering emulsion droplets could be achieved both using UV and visible light which may find interest and applications in various fields such as colloidal engineering, reaction design or for encapsulation purposes.

Acknowledgments

V. Maingret acknowledges support from the Ministère de l'Enseignement Supérieur, de la Recherche et de l'Innovation for his Ph.D. grant. The authors thank their respective academic institution for financial support. The authors also acknowledge Emmanuel Ibarboure for his help in the spatially controlled experiments on fluorescence microscope using visible light and Isabelle Ly for Cryo-SEM observations.

Supporting information

Reaction schemes of the synthesis of Dex-g-PNBA, ^{1}H NMR characterizations of the different products, conversion and DP computations of PNBA-Br, FTIR characterization of PNBA-N_3, SEC chromatograms of PNBA-N_3, Dex-Alkyne and Dex-g-PNBA, modification of dextran and grafting computations, DCR calibration curve, stacked size-distribution curves of

nanoparticle dispersions at t_0 and $t_{3.5months}$, picture of a stable Pickering emulsion after more than 5 months, size measurements of the Pickering emulsions, photo-cleavage scheme of Dex-g-PNBA, irradiation results in different nanoparticle dispersions, irradiation results at half the irradiance, Cryo-SEM pictures, pH 12 adjustment of an irradiated emulsion, Oil volume conservation calculus.

CRediT authorship contribution statement

V. M.: Conceptualization, Investigation, Writing - original draft. **V. S.:** Conceptualization, Writing - review & editing, Supervision. **V. H.:** Conceptualization, Writing - review & editing, Supervision.

References

Bai, R. X., Xue, L. H., Dou, R. K., Meng, S. X., Xie, C. Y., Zhang, Q., Guo, T., & Meng, T. (2016). Light-Triggered Release from Pickering Emulsions Stabilized by TiO2 Nanoparticles with Tailored Wettability. *Langmuir*, *32*(36), 9254–9264. https://doi.org/10.1021/acs.langmuir.6b02329

Chen, Z., Zhou, L., Bing, W., Zhang, Z., Li, Z., Ren, J., & Qu, X. (2014). Light controlled reversible inversion of nanophosphor-stabilized pickering emulsions for biphasic enantioselective biocatalysis. *Journal of the American Chemical Society*, *136*(20), 7498–7504. https://doi.org/10.1021/ja503123m

Del Campo, A., Boos, D., Spiess, H. W., & Jonas, U. (2005). Surface modification with orthogonal photosensitive silanes for sequential chemical lithography and site-selective particle deposition. *Angewandte Chemie - International Edition*, *44*(30), 4707–4712. https://doi.org/10.1002/anie.200500092

Dupont, H., Maingret, V., Schmitt, V., & Héroguez, V. (2021). New Insights into the

Formulation and Polymerization of Pickering Emulsions Stabilized by Natural Organic Particles. *Macromolecules*, *54*(11), 4945–4970. https://doi.org/10.1021/acs.macromol.1c00225

El Founi, M., Soliman, S. M. A., Vanderesse, R., Acherar, S., Guedon, E., Chevalot, I., Babin, J., & Six, J. L. (2018). Light-sensitive dextran-covered PNBA nanoparticles as triggered drug delivery systems: Formulation, characteristics and cytotoxicity. *Journal of Colloid and Interface Science*, *514*, 289–298. https://doi.org/10.1016/j.jcis.2017.12.036

Jiang, J., Ma, Y., Cui, Z., & Binks, B. P. (2016). Pickering Emulsions Responsive to CO2/N2 and Light Dual Stimuli at Ambient Temperature. *Langmuir*, *32*(34), 8668–8675. https://doi.org/10.1021/acs.langmuir.6b01475

Maingret, V., Courrégelongue, C., Schmitt, V., & Héroguez, V. (2020). Dextran-Based Nanoparticles to Formulate pH-Responsive Pickering Emulsions: A Fully Degradable Vector at a Day Scale. *Biomacromolecules*, *21*(12), 5358–5368. https://doi.org/10.1021/acs.biomac.0c01489

Ren, G., Zheng, X., Gu, H., Di, W., Wang, Z., Guo, Y., Xu, Z., & Sun, D. (2019). Temperature and CO2 Dual-Responsive Pickering Emulsions Using Jeffamine M2005-Modified Cellulose Nanocrystals. *Langmuir*, *35*(42), 13663–13670. https://doi.org/10.1021/acs.langmuir.9b02497

Schmitt, V., Destribats, M., & Backov, R. (2014). Colloidal particles as liquid dispersion stabilizer: Pickering emulsions and materials thereof. *Comptes Rendus Physique*, *15*(8–9), 761–774. https://doi.org/10.1016/j.crhy.2014.09.010

Soliman, S. M. A. (2018). *From photosensitive glycopolymers to smart drug delivery systems*.

Soliman, S. M. A., Colombeau, L., Nouvel, C., Babin, J., & Six, J. L. (2016). Amphiphilic photosensitive dextran-g-poly(o-nitrobenzyl acrylate) glycopolymers. *Carbohydrate Polymers*, *136*, 598–608. https://doi.org/10.1016/j.carbpol.2015.09.061

Soliman, S. M. A., El Founi, M., Vanderesse, R., Acherar, S., Ferji, K., Babin, J., & Six, J. L. (2019). Light-sensitive dextran-covered PNBA nanoparticles to continuously or discontinuously improve the drug release. *Colloids and Surfaces B: Biointerfaces*, *182*(May), 110393. https://doi.org/10.1016/j.colsurfb.2019.110393

Soliman, S. M. A., Nouvel, C., Babin, J., & Six, J. L. (2014). O-nitrobenzyl acrylate is polymerizable by single electron transfer-living radical polymerization. *Journal of Polymer Science, Part A: Polymer Chemistry*, *52*(15), 2192–2201. https://doi.org/10.1002/pola.27232

Tajmoradi, Z., Roghani-Mamaqani, H., & Salami-Kalajahi, M. (2021). Cellulose nanocrystal-grafted multi-responsive copolymers containing cleavable o-nitrobenzyl ester units for stimuli-stabilization of oil-in-water droplets. *Chemical Engineering Journal*, *October*, 128005. https://doi.org/10.1016/j.cej.2020.128005

Tang, J., Quinlan, P. J., & Tam, K. C. (2015). Stimuli-responsive Pickering emulsions: Recent advances and potential applications. *Soft Matter*, *11*(18), 3512–3529. https://doi.org/10.1039/c5sm00247h

Xie, C. Y., Meng, S. X., Xue, L. H., Bai, R. X., Yang, X., Wang, Y., Qiu, Z. P., Binks, B. P., Guo, T., & Meng, T. (2017). Light and Magnetic Dual-Responsive Pickering Emulsion Micro-Reactors. *Langmuir*, *33*(49), 14139–14148. https://doi.org/10.1021/acs.langmuir.7b03642

Zeng, T., Deng, A., Yang, D., Li, H., Qi, C., & Gao, Y. (2019). Triple-Responsive Pickering Emulsion Stabilized by Core Cross-linked Supramolecular Polymer Particles. *Langmuir*, *35*(36), 11872–11880. https://doi.org/10.1021/acs.langmuir.9b02341

Zhao, H., Sterner, E. S., Coughlin, E. B., & Theato, P. (2012). O-Nitrobenzyl alcohol derivatives: Opportunities in polymer and materials science. *Macromolecules*, *45*(4), 1723–1736. https://doi.org/10.1021/ma201924h

Zhao, X., Fang, X., Yang, S., Zhang, S., Yu, G., Liu, Y., Zhou, Y., Feng, Y., & Li, J. (2021). Light-tuning amphiphility of host-guest Alginate-based supramolecular assemblies for photo-responsive Pickering emulsions. *Carbohydrate Polymers*, *251*(June 2020), 117072. https://doi.org/10.1016/j.carbpol.2020.117072